J|A|C|S COMMUNICATIONS

Published on Web 04/01/2010

Imaging Structure Sensitive Catalysis on Different Shape-Controlled Platinum Nanoparticles

Carlos M. Sánchez-Sánchez, José Solla-Gullón, Francisco J. Vidal-Iglesias, Antonio Aldaz, Vicente Montiel, and Enrique Herrero*

Departamento de Química Física and Instituto Universitario de Electroquímica, Universidad de Alicante, Ap. 99, 03080 Alicante, Spain

Received February 2, 2010; E-mail: herrero@ua.es

Preferentially oriented, also called, shape-controlled, nanoparticles (NPs) provide the opportunity to demonstrate that heterogeneous catalysis is controlled not only by the chemical composition and size of the catalyst or electrode used[1,2] but also by the type of surface sites available at the catalyst surface.[3] In this communication, we present direct imaging of the different catalytic rates displayed by four different types of shape-controlled platinum NPs catalyzing the oxygen reduction reaction (ORR, reaction 1).

$$O_2 + 4H^+ + 4e \rightarrow 2H_2O \quad (1)$$

Crystallography distinguishes a large variety of sites at the surface of a metallic crystal. Preferentially oriented NPs present specific crystallographic planes at the surface (facets) depending on their shape. Miller indexes are used to define the type of surface from a crystallographic point of view. In particular, platinum presents a face-centered cubic (fcc) crystal structure that only uses three numbers to be defined, *i.e.* (111), (100), and (110) for the three basal planes. When the catalytic properties of a particular material are evaluated, it is easy to forget surface structure differences and only link catalytic activity with size and/or surface composition. But NP shape dependency has been demonstrated as a key factor in several processes such as the electron transfer between hexacyanoferrate (III) and thiosulfate ions in solution where tetrahedral Pt NPs exhibited a 5 times larger rate constant than cubic Pt NPs.[4] Recently, another Pt NP shape (multiarmed nanostar) has been demonstrated to be even more active for this catalytic reaction.[5] Moreover, some gas-phase reactions catalyzed with Pt NPs, such as ethylene and benzene hydrogenations, have been proven activity-sensitive to the NP shape.[6,7]

The synthesis of shape-controlled Pt NPs normally uses the adsorption of organic capping agents for directing the crystal growth by enhancing a particular facet at the NP surface. Polyvinylpyrrolidone (PVP) and polyacrylate (PA) are the most widely used capping agents in shaped-nanoparticle synthesis. Both organic molecules interact strongly through their carbonyl group with the Pt surface blocking some active sites at the Pt surface.[8] Thus, once the type of surface site is controlled through the synthesis it is really important to clean the NPs from the different capping agents employed before studying any catalytic process on their surface. We compare in this work the very different behaviors observed for clean spherical ($PtNP_{sphe}$), cubic ($PtNP_{cubic}$), hexagonal ($PtNP_{hexa}$), and tetrahedral-octahedral ($PtNP_{tetra}$) platinum NPs when the ORR takes place on their surface. We use different colloidal syntheses to obtain these shape-controlled Pt NPs using PA as a capping agent in all cases but spherical NPs, which are synthesized in a water-in-oil microemulsion. Figure 1 shows some representative TEM images of the above-mentioned Pt NPs. Then, we carry out a cleaning procedure with the Pt NPs in an aqueous suspension. Water-in-oil microemulsion synthesis only requires successive acetone, acetone−water mixtures and water washes to achieve a total cleaning of $PtNP_{sphe}$. However, colloidal syntheses require total PA deprotonation in a strong basic medium, followed by several water washes. After cleaning, all four types of Pt NPs agglomerate leading to a heterogeneous suspension with a clear solid−liquid separation. For this reason, it is necessary to sonicate the suspensions before using the NPs for studying the ORR. The cleaning procedure is a key issue when different catalysts are compared because organics acting as capping agents may hinder or totally block the catalysis at the Pt NP's surface, as for instance has been reported for the ethylene hydrogenation reaction when Pt NPs synthesized using PVP are used as a catalyst.[7]

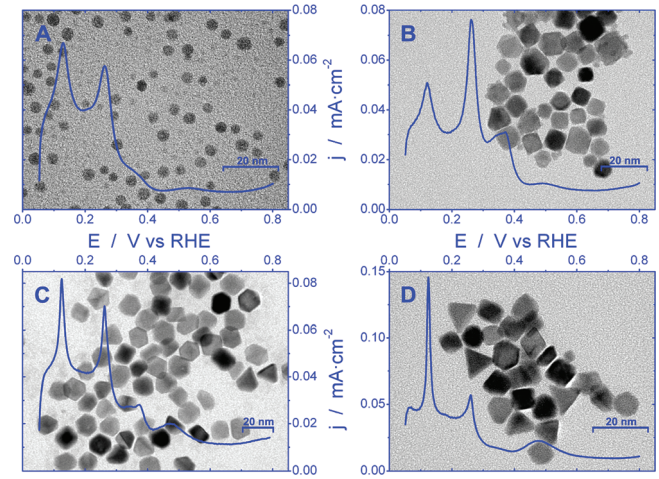

Figure 1. TEM pictures and voltammetric profiles of preferentially (A) spherical ($PtNP_{sphe}$), (B) cubic ($PtNP_{cubic}$), (C) hexagonal ($PtNP_{hexa}$), and (D) tetrahedral-octahedral ($PtNP_{tetra}$) platinum NPs. Voltammograms were performed in oxygen-free 0.5 M H_2SO_4 at 50 mV/s.

We prove the organic-free status of all our Pt NPs with the characteristic hydrogen desorption peaks displayed in the voltammograms shown in Figure 1. Our Pt NPs show those peaks at the same potentials where flame cleaned (111), (110), and (100) single crystal electrodes do. Thus, these peaks provide qualitative information about the nature of the surface sites and represent the electrochemical fingerprint of totally clean Pt.[9,10] For this reason, we present the electrochemical response of each type of Pt NPs at the hydrogen under potential deposition (UPD) region, which would be hindered in the presence of contaminants at the Pt surface. Note the different voltammograms shown in Figure 1 exhibit significant differences in the relative intensity of the hydrogen desorption peaks. This is related to the different shapes of the studied NPs that produce different preferential sites at the Pt surface.[11] Especially

10.1021/ja100922h © 2010 American Chemical Society

difficult to be recognized is the broad peak at 0.5 V due to the contribution from (111) sites which is only evident in $PtNP_{tetra}$ and $PtNP_{hexa}$.

Normalization of the total surface area for each type of NP is another important parameter to control before studying the ORR, since different syntheses give as a result NPs with different average sizes. Table 1 shows the main NP shape, preferential surface facet associated, and average size as evaluated by TEM. It is evident that $PtNP_{sphe}$ are significantly different in size than the other three types of Pt NPs. In spite of that, no size effect below the 3 nm diameter range unrelated to the particle geometry has been reported; that is, the only expected effects in catalysis for the NPs studied here are geometrical effects.

Table 1. Average Size and Preferential Surface Orientation of Different Types of Pt NPs

Main Pt NP shape	Average size (nm)	Preferential surface facets
Tetrahedral-Octahedral ($PtNP_{tetra}$)	8.6 ± 1.4	(111) and (110)
Cubic ($PtNP_{cubic}$)	8.2 ± 1.6	(100)
Spherical ($PtNP_{sphe}$)	4.5 ± 0.8	No preferential facet
Hexagonal ($PtNP_{hexa}$)	11.5 ± 1.7	(100) and (111)

The active surface area of each type of Pt NP was determined electrochemically by the charge involved in the hydrogen UPD region after the subtraction of the double layer contribution and assuming a calibration ratio of 0.21 mC cm^{-2}. This (UPD charge)/(Pt surface area) ratio was established from Pt polycrystalline studies reported in the literature.[12] Once the active surface is evaluated, new aqueous suspensions of the four different Pt NPs are prepared obtaining different NP concentrations but equal active surface areas of Pt (0.045 $cm^2/\mu L$). Then, a Pt NPs array is prepared using equal amounts of these four suspensions.

Electrocatalysis is used in a wide range of applications.[13] In particular, the lack of stable and highly efficient electrocatalysts for the ORR prevents the total development of fuel cells as a useful energy source. Pt NPs are the most common electrocatalyst used, but their long-term performance is still far from being optimized. The tip generation−substrate collection (TG/SC) mode of Scanning Electrochemical Microscopy (SECM)[14] has been successfully used for rapid array imaging of microsized catalysts for the ORR in acid solution.[15] Then, following these well-established procedures for array preparation and screening, we prepared, supported on a glassy carbon plate, a new type of array composed of equal rows of spots with the four types of shape-controlled Pt NPs. This array is scanned in the $X-Y$ plane in a deaerated acid solution with a gold ultramicroelectrode (UME) tip held at a constant anodic current (+150 nA) to generate a constant O_2 flow. The substrate reduction current collected at a given potential when the tip is above a particular spot in the array is an estimation of the ORR catalytic rate of that spot.

SECM images presented in Figures 2 and 3 show two different current contributions. On the one hand, a background current was produced by the array in an oxygen-free solution and represented in green color. On the other hand, the increase in the reduction current was observed when the tip generator is scanned above an active spot for ORR, which is represented in yellow or orange colors. Thus, the different catalytic activities for ORR of all four shape-controlled Pt NPs are shown in Figures 2 and 3. Figure 2 shows images of a Pt NPs array held at two different potentials (0.7 and 0.4 V) in 0.1 M $HClO_4$ solution. In these images the high catalytic activity for ORR is represented by high reduction current values (orange points on the image). At 0.7 V, the kinetic reaction rate for the ORR on platinum is not very high, and therefore, differences in reactivity depending on the NP shape should be observed. On the other hand, at 0.4 V, the kinetic reaction rate is so high that any O_2 molecule arriving at the NPs is immediately reduced, and the current depends only on the diffusion rate of O_2 toward the surface, which is the same in all cases. For that reason, the measured activity at 0.4 V should be basically the same and this experiment can be considered as a control test. As can be seen in Figure 2A, $PtNP_{hexa}$ exhibit the highest activity for ORR at 0.7 V, whereas in the control experiment at 0.4 V (Figure 2B) all four shape-controlled Pt NPs exhibit almost the same activity.

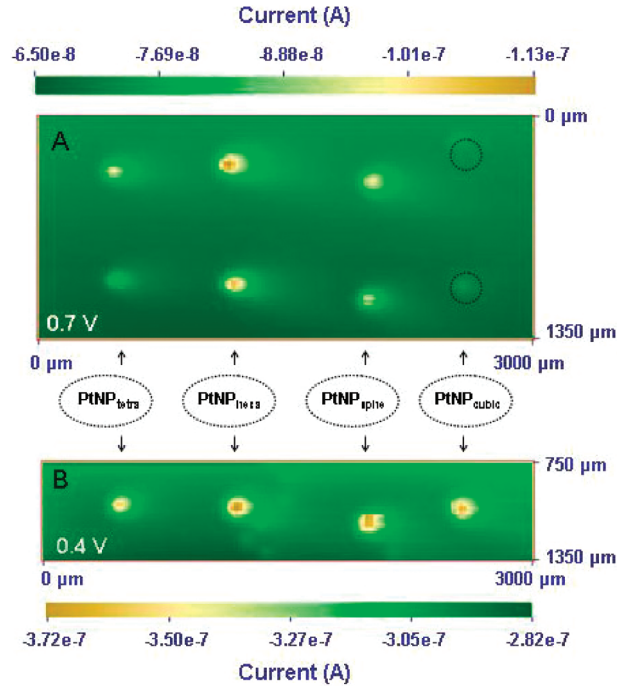

Figure 2. SECM TG/SC images displaying the reduction current collected for ORR in 0.1 M $HClO_4$ solution at a Pt NPs array. This array is formed by spots of four different types of shape-controlled Pt NPs. Scan rate = 125 μm/s. (A) Image of the first and second rows of the array held constant at 0.7 V. (B) Image of the second row of the array held constant at 0.4 V.

SECM imaging is particularly useful to distinguish significant activity differences, but it is not possible to scale $PtNP_{tetra}$ and $PtNP_{sphe}$ from the currents displayed in Figure 2. According to the image shown in Figure 2A at 0.7 V, the activity for the ORR for all four different PtNPs in 0.1 M $HClO_4$ solution is as follows: $PtNP_{hexa} > PtNP_{tetra} \approx PtNP_{sphe} > PtNP_{cubic}$. Since the reactivity for the ORR depends on the anion present in solution, a new image at 0.7 V of an equal but independent array was conducted in 0.5 M H_2SO_4 solution and is shown in Figure 3. In this case, $PtNP_{hexa}$ exhibit again the highest activity for ORR, but $PtNP_{cubic}$ and $PtNP_{tetra}$ show a switch in their activities in comparison with Figure 2A as a consequence of the different anion present in solution. Thus, Figure 3 obtained in sulfuric acid solution gives as a result a different gradation than the one obtained from Figure 2A in perchloric solution. Gradation of all four different PtNPs in 0.5 M H_2SO_4 solution is as follows: $PtNP_{hexa} > PtNP_{cubic} > PtNP_{sphe} > PtNP_{tetra}$. The magnitude of the oxygen reduction current provided by the $PtNP_{cubic}$ spots in Figure 2A and $PtNP_{tetra}$ spots in Figure 3 is not clearly different than the background. For this reason, we include dotted circles in these images to show the location of those spots. These results can be compared to those reported in the

literature for flame cleaned Pt single crystal electrodes with different crystallographic orientations and different anions present in solution.[16,17] In particular, Pt single crystal (111) shows low activity in a sulfuric but high activity in a perchloric medium as has been observed for $PtNP_{tetra}$ in our images (Figures 2A and 3). In contrast, Pt single crystal (100) shows low activity in a perchloric but high activity in a sulfuric medium as has also been observed for $PtNP_{cubic}$ in our images (Figures 2A and 3). Therefore, the preferential (111) surface facets at $PtNP_{tetra}$ and (100) at $PtNP_{cubic}$ (see Table 1) are responsible for this noticeable switch in activity for ORR as a function of the anion present in solution. On the other hand, $PtNP_{hexa}$ benefits from having both types of sites which can work in either perchloric or sulfuric media.

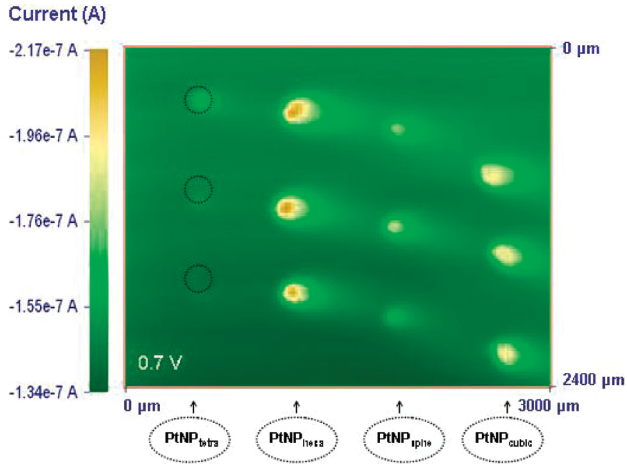

Figure 3. SECM TG/SC image displaying the reduction current collected for ORR in 0.5 M H_2SO_4 solution at a Pt NPs array. This array presents three equal rows composed by spots of four different types of shape-controlled Pt NPs, and its potential is held constant at 0.7 V. Scan rate = 125 μm/s.

To prove that the only effects reported here are those associated with the different geometries of the samples, the surface structure of the NPs was electrochemically disordered. Figure 4A and 4B show SECM images comparing all four types of Pt NPs in a fresh array at 0.7 V in sulfuric solution before and after undergoing an in situ oxidation step at 1.4 V followed by a reduction step at 0.7 V, respectively. Figure 4A shows the same activity trend already displayed in Figure 3. In contrast, Figure 4B shows equal activity for all four spots (dispersion <5%) after Pt surface reconstruction. This oxidation−reduction process removes all specific crystallographic features at the Pt surface and gives as a result high step density NPs with no preferential facets. This process also increases the Pt NPs' roughness and surface area, which increases the maximum current collected at the spots in comparison with Figure 4A. Thus, these images point out no significant size effect in ORR catalysis for the Pt NPs studied.

In conclusion, this work presents direct observation by SECM imaging of different catalytic activities for four different shape-controlled Pt NPs catalyzing the same reaction (ORR, reaction 1) in two different acid electrolytes (0.1 M $HClO_4$ and 0.5 M H_2SO_4). This demonstrates surface structure dependency at the nanoscale level in the catalysis of one of the most relevant electrochemical reactions for energy conversion. Moreover, we have been able to grade the activity of the different shape-controlled Pt NPs and correlate our imaging results with previous single crystal electrode studies setting a linkage between reactivity and well-defined surface

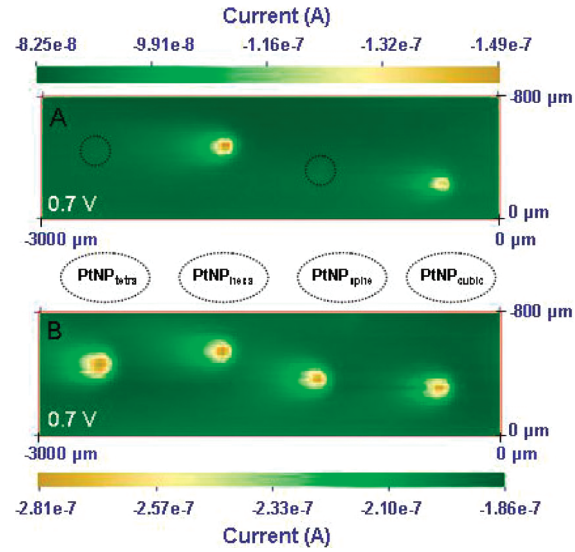

Figure 4. SECM TG/SC image displaying the reduction current collected for ORR in 0.5 M H_2SO_4 solution at a Pt NPs array. This array presents four different types of shape-controlled Pt NPs. Scan rate = 125 μm/s. (A) Image of a fresh array held constant at 0.7 V. (B) Image of the same array after oxidation at 1.4 V for 30 min and further reduction at 0.7 V for 1 h.

geometry at NPs. These results show the importance of the effective control of the NP shape in catalysis and not only of the NP size and atomic composition.

Acknowledgment. This work has been financially supported by Ministerio de Educación y Ciencia-FEDER, CTQ2006-04071/BQU.

Supporting Information Available: Experimental details describing: NPs syntheses, characterization and area normalization, TEM analyses, array preparation and SECM imaging. This material is available free of charge via the Internet at http://pubs.acs.org.

References

(1) Xiao, X.; Bard, A. J. *J. Am. Chem. Soc.* **2007**, *129*, 9610.
(2) Wilson, O. M.; Knecht, M. R.; Garcia-Martinez, J. C.; Crooks, R. M. *J. Am. Chem. Soc.* **2006**, *128*, 4510.
(3) Solla-Gullón, J.; Vidal-Iglesias, F. J.; López-Cudero, A.; Garnier, E.; Feliu, J. M.; Aldaz, A. *Phys. Chem. Chem. Phys.* **2008**, *10*, 3689.
(4) Narayanan, R.; El-Sayed, M. A. *Nano Lett.* **2004**, *4*, 1343.
(5) Mahmoud, M. A.; Tabor, C. E.; El-Sayed, M. A.; Ding, Y.; Wang, Z. L. *J. Am. Chem. Soc.* **2008**, *130*, 4590.
(6) Bratlie, K. M.; Lee, H.; Komvopoulos, K.; Yang, P.; Somorjai, G. A. *Nano Lett.* **2007**, *7*, 3097.
(7) Lee, H.; Habas, S. E.; Kweskin, S.; Butcher, D.; Somorjai, G. A.; Yang, P. *Angew. Chem., Int. Ed.* **2006**, *45*, 7824.
(8) Borodko, Y.; Habas, S. E.; Koebel, M.; Yang, P.; Frei, H.; Somorjai, G. A. *J. Phys. Chem. B* **2006**, *110*, 23052.
(9) Clavilier, J. In *Interfacial Electrochemistry; Theory, Experiment and Applications*; Wieckowski, A., Ed.; Marcel Dekker: New York, 1999.
(10) Clavilier, J.; Faure, R.; Guinet, G.; Durand, R. *J. Electroanal. Chem.* **1980**, *107*, 205.
(11) Solla-Gullón, J.; Rodríguez, P.; Herrero, E.; Aldaz, A.; Feliu, J. M. *Phys. Chem. Chem. Phys.* **2008**, *10*, 1359.
(12) Woods, R. In *Electroanalytical Chemistry*, Vol. 9; Bard, A. J., Ed.; Marcel Dekker: New York, 1976.
(13) *Electrocatalysis*; Lipkowski, J., Ross, P. N., Eds; Wiley-VCH: New York, 1998.
(14) *Scanning Electrochemical Microscopy*; Bard, A. J., Mirkin, M. V., Eds; Marcel Dekker: New York, 2001.
(15) Fernández, J. L.; Walsh, D. A.; Bard, A. J. *J. Am. Chem. Soc.* **2005**, *127*, 357.
(16) Markovic, N. M.; Adzic, R. R.; Cahan, B. D.; Yeager, E. B. *J. Electroanal. Chem.* **1994**, *377*, 249.
(17) Markovic, N. M.; Gasteiger, H. A.; Ross, P. N. *J. Phys. Chem.* **1995**, *99*, 3411.

JA100922H